TISSUE ENGINEERING: Part A
Volume 21, Numbers 3 and 4, 2015

DOI: 10.1089/ten.tea.2013.0740

Dual-Phase Osteogenic and Vasculogenic Engineered Tissue for Bone Formation

Rameshwar R. Rao, PhD, Marina L. Vigen, MS, Alexis W. Peterson, BS, David J. Caldwell, MSE, Andrew J. Putnam, PhD, and Jan P. Stegemann, PhD

Minimally invasive, injectable bone tissue engineering therapies offer the potential to facilitate orthopedic repair procedures, including in indications where enhanced bone regeneration is needed for complete healing. In this study, we developed a dual-phase tissue construct consisting of osteogenic (Osteo) and vasculogenic (Vasculo) components. A modular tissue engineering approach was used to create collagen/fibrin/hydroxyapatite (COL/FIB/HA) hydrogel microbeads containing embedded human bone marrow-derived mesenchymal stem cells (bmMSC). These microbeads were predifferentiated toward the osteogenic lineage *in vitro* for 14 days, and they were then embedded within a COL/FIB vasculogenic phase containing a coculture of undifferentiated bmMSC and human umbilical vein endothelial cells (HUVEC). *In vitro* studies demonstrated homogenous dispersion of microbeads within the outer phase, with endothelial network formation around the microbeads over 14 days in the coculture conditions. Subcutaneous injection into immunodeficient mice was used to investigate the ability of dual-phase (Osteo + Vasculo) and control (Osteo, Vasculo, Blank) constructs to form neovasculature and ectopic bone. Laser Doppler imaging demonstrated blood perfusion through all constructs at 1, 4, and 8 weeks postimplantation. Histological quantification of total vessel density showed no significant differences between the conditions. Microcomputed tomography indicated significantly higher ectopic bone volume (BV) in the Osteo condition at 4 weeks. At 8 weeks both the Osteo and Blank groups exhibited higher BV compared to the Vasculo and dual Osteo + Vasculo groups. These data not only show that osteogenic microbeads can be used to induce ectopic bone formation, but also suggest an inhibitory effect on BV when undifferentiated bmMSC and HUVEC were included in dual-phase constructs. This work may lead to improved methods for engineering vascularized bone tissue, and to injectable therapies for the treatment of orthopedic pathologies in which bone regeneration is delayed or prevented.

Introduction

A MAIN GOAL IN MUSCULOSKELETAL tissue engineering is the regeneration of bone, and in particular to develop methods for improved healing of recalcitrant bone fractures and large defects. The treatment of such conditions is a serious clinical problem, and a significant number of fractures are complicated by delayed and/or incomplete healing. Many bone tissue engineering strategies aim to recapitulate the native structure of bone by combining cells, materials, and signaling molecules in defined architectures. The primary structural matrix of bone consists of a collagenous extracellular matrix mineralized by hydroxyapatite (HA).[1] However, bone tissue also contains a rich vascular supply, which is vital to satisfying its high metabolic demand.[2] Therefore, both the osseous and the vascular components of bone are critical to forming functional tissue, and bone healing requires concomitant development of both components. This need for a blood supply to nourish newly forming bone has motivated a variety of approaches to engineering vascularized bone tissue.

Controlled delivery of multiple growth factors is one strategy to achieve regeneration of vascularized bone tissue, though the results have been mixed. Patel *et al.* codelivered bone morphogenetic protein-2 (BMP-2) and vascular endothelial growth factor (VEGF) in an orthotopic rat critical size defect model.[3] The dual (BMP-2 + VEGF) group exhibited significantly higher bone volume (BV) percentage as measured by microcomputed tomography (μCT) at 4 weeks compared with the other conditions, but was not statistically different from the other groups at 12 weeks. In later work by the same group, the doses of each of the growth factors were varied in an attempt to reduce BMP-2 concentration while achieving comparable bone formation, however, the codelivery of BMP-2 and VEGF did not result in an increase in bone formation compared to BMP-2 alone.[4] In another

Department of Biomedical Engineering, University of Michigan, Ann Arbor, Michigan.

study, Shah *et al.* evaluated the use of polyelectrolyte films to control delivery rates of BMP-2 and VEGF and demonstrated enhanced bone formation measured by μCT in the dual delivery group, compared with BMP-2 alone at 9 weeks.[5] Similarly, genetic modification of bone marrow-derived mesenchymal stem cells (bmMSC) for the constitutive delivery of both BMP-2 and VEGF demonstrated enhanced healing in the dual group compared with either growth factor alone.[6] These studies have demonstrated the potential promise of dual growth factor release, but the approach is hampered by the complexity of controlling dosing and obtaining the needed temporal release profile.[7–10]

Cell-based approaches to vascularized bone tissue engineering also are being pursued.[11–13] Numerous studies have shown that coculture of endothelial cells and osteogenic cells allows the formation of both vascular networks and mineralized tissue postimplantation. Kaigler *et al.* implanted poly(lactide-co-glycolide) (PLGA) scaffolds containing a coculture of human microvascular endothelial cells (HMVEC) and bmMSC into immunodeficient mice and monitored ectopic bone formation over 8 weeks.[14] Total vasculature was similar in the implants containing both cell types (bmMSC + HMVEC) compared to the bmMSC alone, but bone formation was significantly higher in the dual cell condition compared with bmMSC alone. Usami *et al.* also demonstrated ectopic bone formation through the cotransplantation of endothelial progenitor cells (EPC) and bmMSC on collagen fiber meshes.[15] Both neovasculature and bone formation were significantly higher in the bmMSC + EPC group at 12 weeks postimplantation.

Orthotopic models have also been used to demonstrate osteogenesis induced by transplant of multiple cell types. Grellier *et al.* delivered alginate microspheres seeded with human umbilical vein endothelial cells (HUVEC) and bmMSC into a femoral defect model in immunocompromised mice.[16] Enhanced bone regeneration was observed in the dual condition (bmMSC + HUVEC) compared to the bmMSC group alone. In an attempt to look at the effects of predifferentiation, Tsigkou *et al.* first seeded bmMSC on PLGA scaffolds and then cultured the cell-seeded scaffolds for 1 week in osteogenic supplemented medium to induce differentiation.[17] The scaffold was then coated with a collagen/fibronectin hydrogel containing bmMSC and HUVEC and subcutaneously implanted into immunodeficient mice. Both perfused human vasculature and bone formation were observed after 8 weeks postimplantation, suggesting an added benefit to predifferentiating bmMSC prior to implantation in forming vascularized bone tissue.

The goal of this study was to evaluate the effectiveness of a minimally invasive, injectable, dual-phase tissue engineering approach to the regeneration of vascularized bone, as shown schematically in Figure 1. Our laboratory has previously employed modular tissue engineering techniques to fabricate three-dimensional (3D) cell-seeded hydrogel ''microbeads'' comprised of physiologically relevant proteins and polysaccharides, and has shown that they can be used as microenvironments to support osteogenic differentiation of embedded bmMSC.[18,19] We have also shown that composite matrices formed from collagen and fibrin (COL/FIB) support the formation of vessel-like structures when seeded with a defined coculture of bmMSC and HUVEC.[20] In this work, we have combined osteogenically differentiated bmMSC-seeded COL/FIB/HA microbeads with a COL/FIB matrix containing both bmMSC and HUVEC. We performed *in vitro* studies to examine vessel network formation around the microbeads, and *in vivo* experiments to measure ectopic bone formation in a subcutaneous injection model in immunocompromised mice. This dual-phase

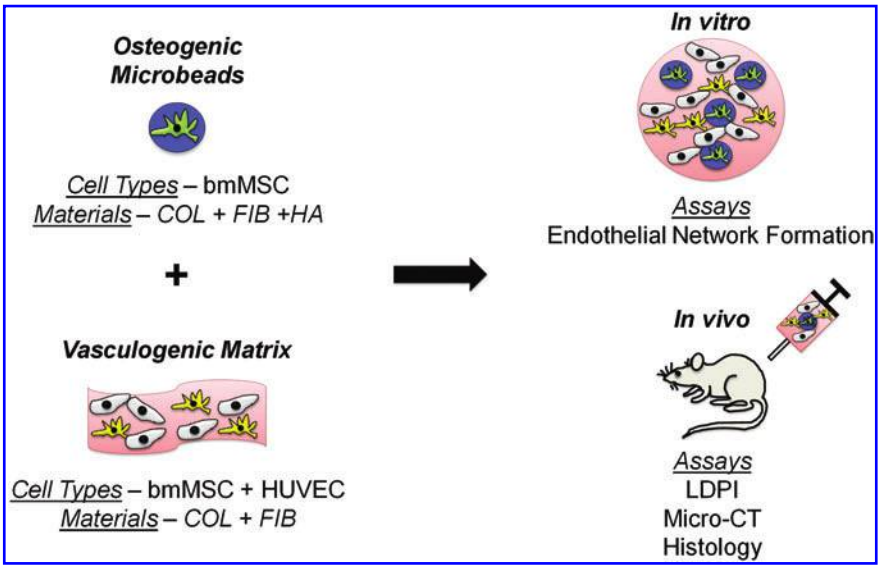

FIG. 1. Schematic of the design and fabrication of dual-phase engineered tissues. Modular microbeads consisting of bmMSC (*green*) in a COL/FIB/HA matrix (*blue*) were fabricated and cultured in osteogenic medium for 14 days. Microbeads were then combined within a surrounding COL/FIB matrix (*pink*) containing a coculture of HUVEC (*yellow*) and undifferentiated bmMSC (*gray*). *In vitro* studies were performed to investigate endothelial network formation around the osteogenic microbeads. *In vivo* studies were performed to monitor neovascularization and ectopic bone formation in a subcutaneous model in the mouse. bmMSC, bone marrow-derived mesenchymal stem cells; COL/FIB/HA, collagen/fibrin/hydroxyapatite; HUVEC, human umbilical vein endothelial cells. Color images available online at www.liebertpub.com/tea

microbead-hydrogel approach is initially targeted at non-load-bearing applications such as tumor resections and other cavitary defects, though it could be combined with mechanical fixation methods for application to load-bearing defects. The development of injectable and modular methods to potentiate the formation of vascularized bone would be an important advance in tissue engineering, and would have an impact on a variety of clinical pathologies in which bone healing is delayed or incomplete.

Materials and Methods

Cell culture

Human bmMSC (Lonza, Inc.) were cultured in alpha-minimum essential media (α-MEM; Life Technologies) supplemented with 10% bmMSC-qualified fetal bovine serum (FBS; Life Technologies) and 1% penicillin and streptomyocin (Life Technologies). The bmMSC in this study were from a 19-year-old female and were tested for osteogenic capacity in culture prior to use. bmMSC were used between passages 6–8 with media changes every other day. HUVEC were isolated from umbilical cords as previously described.[20] HUVEC were cultured in endothelial growth media-2 (EGM-2; Lonza, Inc.) and used between passages 4–5. Culture medium was changed every other day.

Fabrication of osteogenic microbeads

COL/FIB/HA composite microbeads were fabricated as previously described.[19] Briefly, bovine type I COL (MP Biomedicals) was dissolved at a concentration of 4.0 mg/mL in 0.02 N acetic acid. Bovine fibrinogen (FIB; Sigma Aldrich) was dissolved in serum-free Dulbecco's modified Eagle's medium (DMEM; Thermo Scientific) at 4.0 mg/mL clottable protein. COL and FIB were combined to yield a total protein concentration of 2.5 mg/mL (mass ratio 50/50) and added to a mixture containing 2% bovine thrombin (1 U/mL; Sigma), 1.0 mM glyoxal (Sigma), 5% 0.1 N NaOH, 10% 5×-concentrated DMEM, 10% FBS, and 2.5 mg/mL of nano-HA (Sigma) at 4°C. HA was sonicated for 1 h prior to use to maintain homogenous distribution of the particles after microbead encapsulation.[21] Cells were directly added into the gel mixture to guarantee their uniform distribution within the microbeads. The mixture was then injected into a bath of 100 cSt polydimethylsiloxane (Xiameter; Dow Corning) that was cooled to 0°C and stirred at 600 rpm for 5 min with a double-bladed impeller. The temperature was then increased to 37°C, inducing gelation of COL and FIB and formation of composite microbeads with embedded bmMSC. Collection of microbeads from the oil phase was performed by centrifuging the mixture at 200 *g* for 5 min and washing with phosphate-buffered saline (PBS; Life Technologies) supplemented with Pluronic L101 (BASF). Microbeads were cultured and maintained in α-MEM supplemented with 2.0 mg/mL ε-amino caproic acid (ACA; Sigma) to prevent fibrinolysis. Media was changed every other day. Acellular microbeads were stained with EZBlue Coomasie reagent and visualized with a light microscope (Olympus America).[19] Acellular microbeads were also labeled with 5 μg/mL FITC-fibrinogen (Life Technologies) at the time of microbead fabrication to visualize dispersion within COL/FIB hydrogels.

Osteogenic differentiation of microbeads

Cell-seeded microbeads were induced to differentiate toward the osteogenic lineage by culturing the microbeads for 14 days in α-MEM supplemented with 2.0 mg/mL ACA, 50 μg/mL ascorbic acid 2-phosphate (Sigma), 10 mM β-glycerophosphate (Sigma), and 100 nM dexamethasone (Sigma). Microbeads were collected by centrifugation at 200 *g* for 5 min prior to the media change.

Fabrication of vasculogenic matrix

Composite COL/FIB hydrogels were fabricated as previously described to serve as a vasculogenic surrounding matrix for the microbeads.[20] Both cell-seeded and acellular microbeads were encapsulated directly into the vasculogenic gel mixture at a ratio of 1:1 microbead-hydrogel mixture by centrifuging the microbeads for 5 min at 200 *g* and then removing the excess media. COL and FIB (total protein concentration of 2.5 mg/mL and a mass ratio of 40/60) were then added at 4°C to 2% bovine thrombin (1 U/mL), 5% 0.1 N NaOH, 10% 5×-concentrated DMEM, 10% FBS, and serum-free EGM-2 to bring the final volume to 100%. The mixture was then transferred into a 24-well plate and allowed to gel for 30 min. Four conditions were used throughout the study as listed in Table 1. For bmMSC-HUVEC coculture conditions, both cell types were added into the gel mixture at 300,000 cells/mL (600,000 total cells/mL) at a 1:1 cell ratio. EGM-2 was added on top of the gels and cell-seeded gels were cultured at 37°C and 5% CO_2. Media was changed every other day. A summary of the *in vitro* cell concentrations and conditions is shown in Table 1.

Immunofluorescent staining

At days 7 and 14, cell-seeded microbeads and hydrogels were washed twice in PBS for 5 min/wash and then fixed in zinc-buffered formalin (Z-Fix; Anatech) for 10 min at 4°C. After two subsequent washes in PBS, embedded cells were

Table 1. Explanation of Microbead and Hydrogel Composition Used for *In Vitro* Studies

	COL/FIB/HA microbeads	*COL/FIB hydrogel*
Blank	Acelluar	Acelluar
Vasculo	Acellular	3×10^5 bmMSC/mL + 3×10^5 HUVEC/mL
Osteo	1×10^6 bmMSC/mL	Acellular
Osteo + Vasculo	1×10^6 bmMSC/mL	3×10^5 bmMSC/mL + 3×10^5 HUVEC/mL

bmMSC, bone marrow-derived mesenchymal stem cells; COL/FIB/HA, collagen/fibrin/hydroxyapatite; HUVEC, human umbilical vein endothelial cells.

permeabilized with 0.5% Triton X-100 (Sigma) in PBS for 20 min at room temperature. Gels were then washed again twice in PBS for 5 min/wash, and the appropriate stain was added at room temperature. Stains were added to 1% bovine serum albumin (Sigma) in PBS at the appropriate concentration: 165 nM AlexaFluor 488 phalloidin (Life Technologies), 20 μg/mL rhodamine labeled Ulex Europaeus Agglutinin I (UEA-1; Vector Laboratories), and 10 nM fluorescent DAPI (Life Technologies). Gels were then washed twice in PBS prior to imaging on a confocal microscope (Nikon Instruments, Inc.).

Implantation into subcutaneous site in the mouse

All animal experiments were performed in accordance with the National Institutes of Health Guidelines and by following a protocol approved by the University of Michigan's Committee on Use and Care of Animals. Male C.B.-17/SCID mice (Taconic Labs) were anesthetized via intraperitoneal injection of a drug cocktail containing ketamine (95 mg/kg; Fort Dodge Animal Health), buprenorphine (0.059 mg/kg; Bedford Laboratories), and xylazine (9.5 mg/kg; Lloyd Laboratories). The injection site on the dorsal surface of the mouse was then shaved and sterilized with betadine (Thermo Fisher Scientific) and alcohol prior to injection. Microbeads were added into the hydrogel mixture at a ratio of 1:1 microbead-hydrogel and the total cell concentration was increased relative to the *in vitro* studies to 10.0×10^6 cells/mL for the bmMSC-HUVEC coculture conditions (Osteo + Vasculo and Vasculo). A higher cell concentration was used in this phase of the study to be comparable to previous *in vivo* studies that have demonstrated the presence of transplanted perfused human vasculature.[22,23] Table 2 shows a summary of the cell concentrations used with each condition. The external hydrogel carrier was used for all samples. In the Vasculo and Osteo + Vasculo conditions the external hydrogels contained bmMSC and HUVEC, while in the Blank and Osteo conditions the external hydrogel was acellular. Two microbead-hydrogel implants per animal were subcutaneously injected in the dorsal region. The final volume of each sample was 300 μL. Mice were kept stationary for 2 min after injection to allow full gelation of the hydrogel matrix, and they were then placed in fresh cages. Implanted samples were visible and palpable immediately after injection, and remained in place over the 8-week study period.

Laser Doppler perfusion imaging

Blood flow through the implant was imaged noninvasively using laser Doppler perfusion imaging (LDPI; Perimed AB).[22] After sedation as previously described, mice were imaged in triplicate. A region of interest was drawn over the implant area and the mean perfusion through each implant was calculated. Results are represented as fold change from perfusion values before implantation (baseline).

μCT imaging

Ectopic bone formation was measured using μCT imaging (μCT100 Scanco Medical). Explanted tissues were first embedded in 1% agarose and placed in a 34 mm diameter tube and scanned over the entire length of the specimen. Scan settings were set to voxel size 15 μm, 55 kVp, 109 μA, 0.5 mm AL filter, and integration time 500 ms. The threshold used to identify bone was uniformly set at 16% (160 on a grayscale of 0–1000), based on a baseline value obtained from HA mineral placed directly on the scanner. Therefore, all minerals that were observed arose through ectopic mineralization. The volume of tissue volume included in the analysis comprised the entirety of the excised implant including the outer COL/FIB hydrogel. Analysis of the BV (mm^3) and tissue mineral density (TMD; mg/cm^3) of each sample was performed using the manufacturer's software.

Histology

Harvested samples were paraffin embedded, sectioned, and stained with hematoxylin and eosin and von Kossa at the Histology Core Facility at the University of Michigan Dental School. Human cell staining was performed using a human UEA-1 staining kit per manufacturer's instructions (Vector Laboratories). Total vessel density was quantified by manually quantifying representative images of each sample in five distinct areas of the implant. Vessels were defined as structures with lumens containing erythrocytes.

Statistical analysis

All values are presented as mean ± standard deviation. $n = 5$ samples for *in vivo* samples. Statistical significance was set to $p < 0.05$ and was determined by a one-way analysis of variance (ANOVA) test with a protected Fisher's least significant difference test.

Results

Dispersion of microbeads within COL/FIB hydrogels

Figure 2 shows acellular COL/FIB/HA microbeads in suspension (Fig. 2A), and fluorescently labeled acellular COL/FIB/HA microbeads dispersed within COL/FIB hydrogels (Fig. 2B, C). Microbeads exhibited a generally spheroidal morphology immediately after fabrication, and retained their shape over the 2-week culture period. The average microbead diameter was approximately 130 μm, and the large majority of microbeads were in the range of 50–250 μm in diameter. Mild aggregation of microbeads

Table 2. Explanation of Microbead and Hydrogel Composition Used for *In Vivo* Studies

	COL/FIB/HA microbeads	*COL/FIB hydrogel*
Blank	Acelluar	Acelluar
Vasculo	Acelluar	5×10^6 bmMSC/mL + 5×10^6 HUVEC/mL
Osteo	1×10^6 bmMSC/mL	Acellular
Osteo + Vasculo	1×10^6 bmMSC/mL	5×10^6 bmMSC/mL + 5×10^6 HUVEC/mL

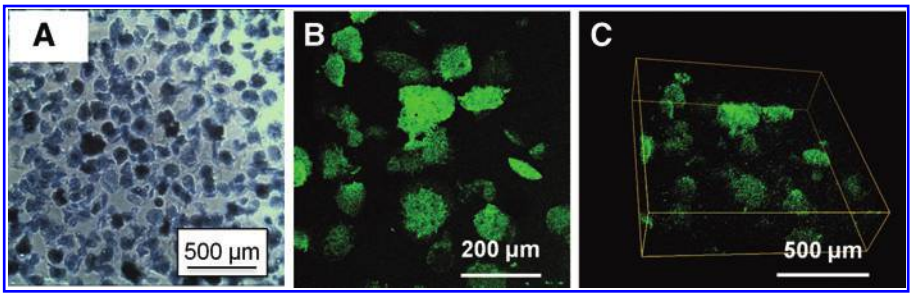

FIG. 2. Light micrograph of **(A)** acellular COL/FIB/HA microbeads, and **(B)** FITC-labeled COL/FIB/HA microbeads dispersed in a COL/FIB hydrogel. **(C)** A 3D reconstruction of the dispersed microbeads. 3D, three-dimensional. Color images available online at www.liebertpub.com/tea

occurred over time when cultured as high density populations; however, microbeads were easily dispersed by gentle pipetting. When embedded in a surrounding COL/FIB hydrogel, microbeads were uniformly distributed within the gel volume (Fig. 2B) and did not aggregate. A 3D reconstruction of the corresponding Z-stack also showed even distribution of microbeads in the Z-axis (Fig. 2C).

Formation of endothelial networks around microbeads in vitro

The generation of vessel-like structures at day 14 around COL/FIB/HA microbeads embedded in COL/FIB hydrogels is shown in Figure 3. The locations of microbeads are indicated by ''MB'' in the image. UEA-1, a human endothelial cell marker, was used to stain vessel networks. Phalloidin served to label the actin cytoskeleton of both the bmMSC and HUVEC, and DAPI showed the nuclei of all cells. Both the Vasculo and Osteo + Vasculo conditions treatments showed clear evidence of the formation of vessel-like structures after 2 weeks in culture, as evidenced by positive UEA-1 staining of cell networks. Colocalization of bmMSC and HUVEC was observed in both of these conditions (positive staining for actin and UEA-1 indicates HUVEC, whereas positive actin stain not associated with UEA-1 indicates bmMSC). The colocalization of the two cell types *in vitro* suggests peri-endothelial interaction between the two cell types in the composite hydrogel. Neither the Blank

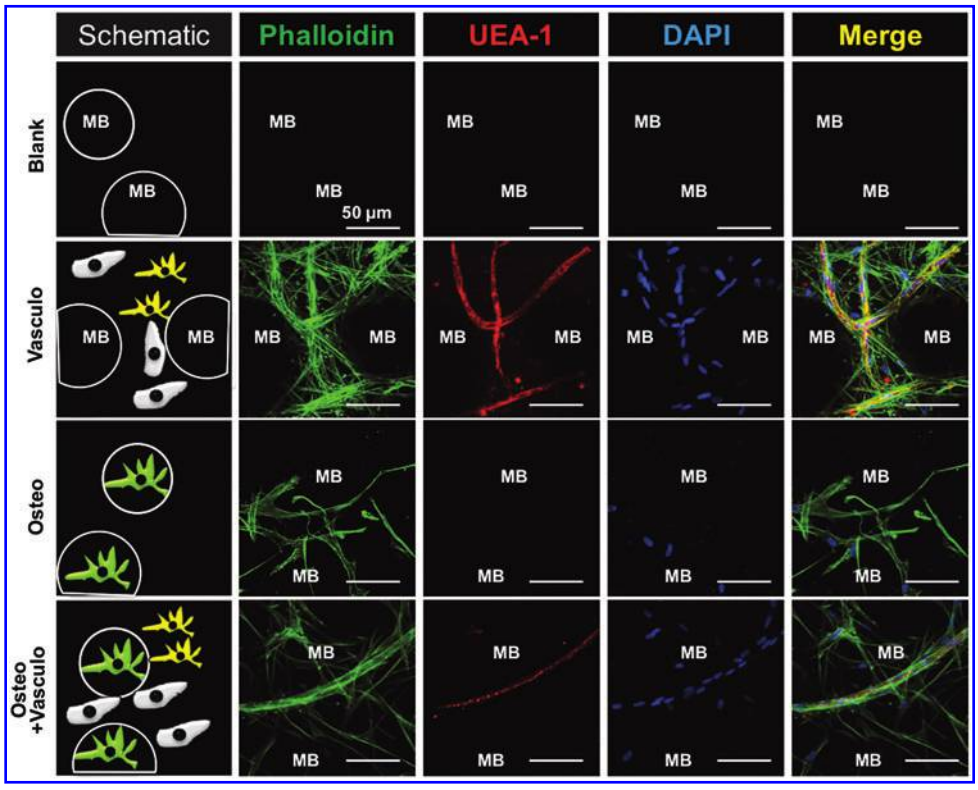

FIG. 3. Vessel-like structure formation around microbeads *in vitro*. Table 1 explains the sample composition. The Blank condition consisted of acellular microbeads embedded in an acellular hydrogel. Vasculo samples consisted of acellular microbeads in a hydrogel containing bmMSC and HUVEC. The Osteo condition consisted of osteogenically differentiated bmMSC-seeded microbeads embedded in an acellular hydrogel. The Osteo + Vasculo condition consisted of osteogenically differentiated bmMSC-seeded microbeads embedded in a hydrogel containing bmMSC and HUVEC. *Green* labeling (phalloidin) shows the actin cytoskeleton of all cells. *Red* labeling (UEA-1) is specific for endothelial cells. *Blue* labeling (DAPO) shows the nuclei of all cells. ''MB'' indicates the location of microbeads. Scale bar = 50 μm. UEA-1, Ulex Europaeus Agglutinin I. Color images available online at www.liebertpub.com/tea

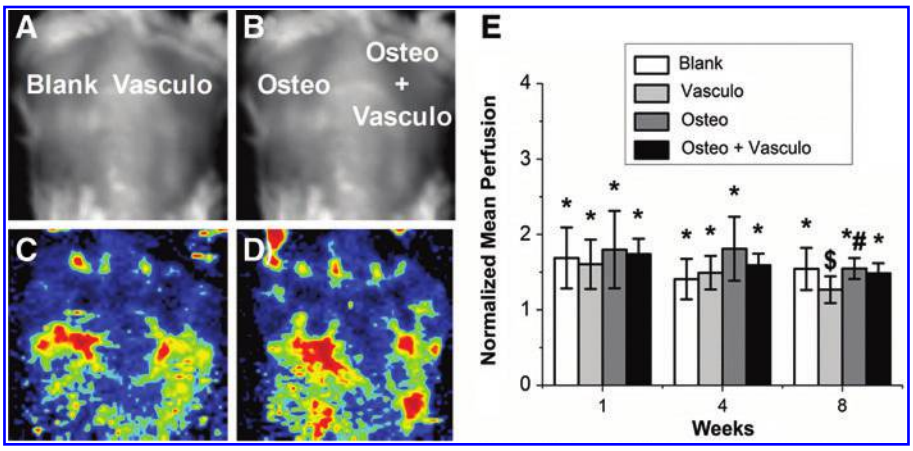

FIG. 4. Laser Doppler Perfusion Imaging. Representative **(A, B)** light images of dorsal implants and **(C, D)** heat maps representing perfusion through the implants at 8 weeks. **(E)** Quantification of mean perfusion normalized to pre-implant. *Statistically significant versus perfusion before implantation. #Statistically significant versus Vasculo. $Statistically significant versus Osteo. Color images available online at www.liebertpub.com/tea

(acellular) nor the Osteo condition exhibited positive UEA-1 staining or vessel-like structures.

Neovascularization of osteogenic-vasculogenic constructs in vivo

Subcutaneous injection of osteogenic microbeads suspended in vasculogenic matrix was used to evaluate the degree of both neovascularization and ectopic bone formation generated by implanted hydrogels. LDPI provided noninvasive measurements of blood flow throughout the implant over the 8-week time course (Fig. 4). A baseline of vascular perfusion was taken before implantation and used to normalize all values at all time points. Perfusion was significantly higher ($p < 0.05$) in all conditions at both 1 and 4 weeks postimplantation, compared with the preimplant baseline. At 8 weeks postimplantation, perfusion values in all conditions except the Vasculo samples remained significantly higher than the baseline, indicating constant perfusion through the implant site. There were no significant differences in perfusion between any of the conditions at any of the time points, except between the Vasculo and Osteo conditions at 8 weeks.

Histological analysis of explanted tissues was also used to examine the degree of vascularization and neovessel formation. Vessel density was quantified at both 4 and 8 weeks and showed no significant differences between any of the conditions at either time point (Fig. 5). The transplantation of bmMSC-HUVEC cocultures did not enhance the degree of vascularization compared to the control Blank (acellular) condition or to the Osteo alone group. Further, there was little evidence of positive staining for human UEA-1 in the Osteo + Vasculo and the Vasculo conditions at 4 weeks (Fig. 6). Degradation of the microbead and hydrogel matrix was not specifically measured in this study, due to the difficulty in positively identifying the originally implanted materials in the histological samples. However, the implants were visible and palpable throughout the implantation period. Histology indicated infiltration of the implant sites by host cells, and the early stages of matrix turnover, concomitant with vascularization and mineralization.

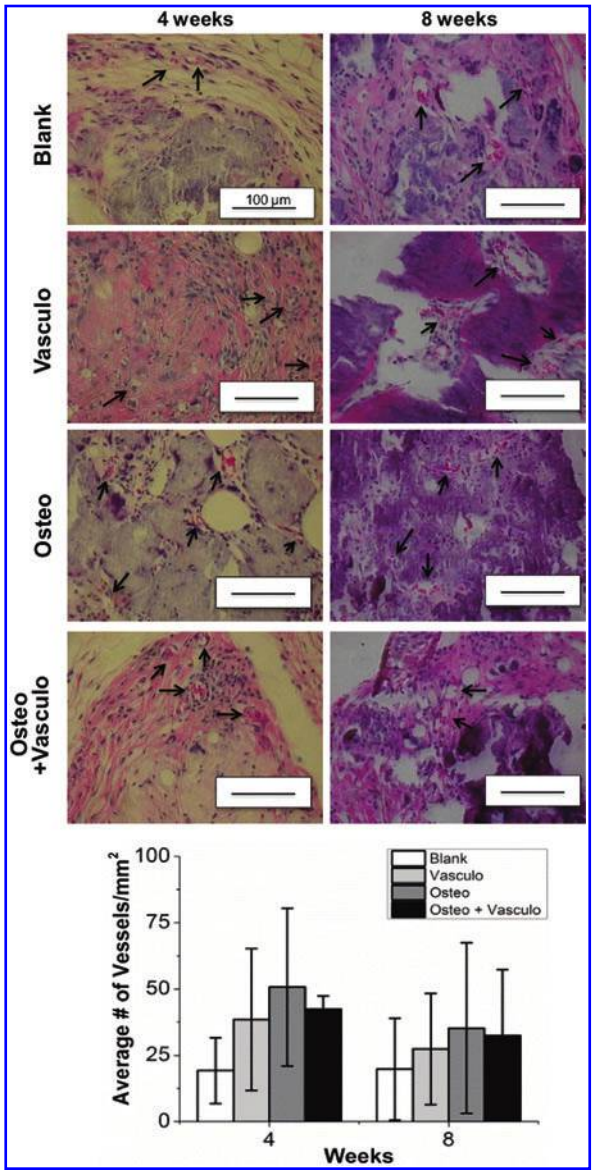

FIG. 5. Histology of samples at 4 and 8 weeks post-implantation. Quantification of erythrocyte-containing vessels (*arrows*) showed no significant differences between any of the conditions at either time point (graph). Scale bar = 100 μm. Color images available online at www.liebertpub.com/tea

Ectopic bone formation

μCT was used as a method to nondestructively image and quantify BV and TMD of explanted tissues (Fig. 7). At 4

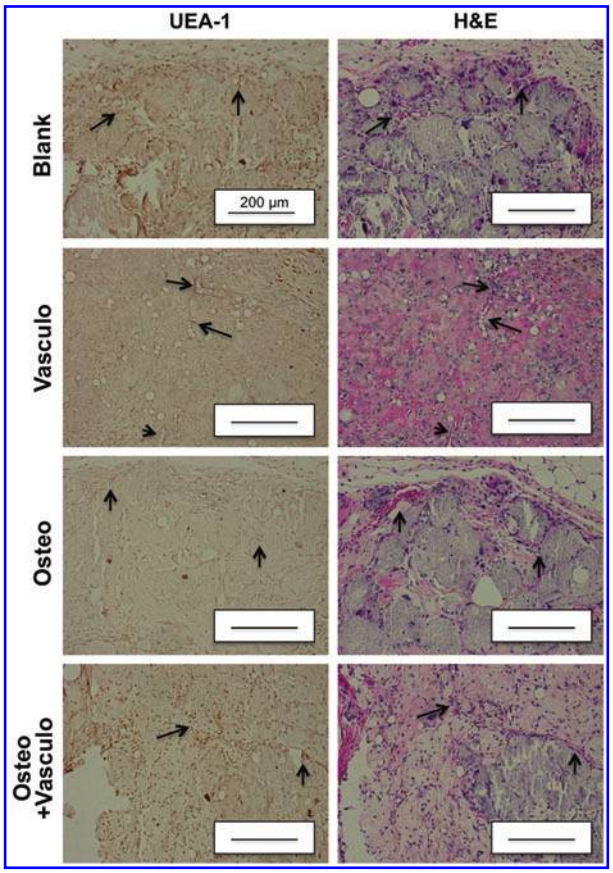

FIG. 6. Staining with human UEA-1 and H&E at 4 weeks. *Arrows* indicate corresponding vasculature in the UEA-1 and H&E slides. Scale bar = 200 μm. H&E, hematoxylin and eosin. Color images available online at www.liebertpub.com/tea

weeks, there were no significant differences between the BV of the Blank, Vasculo, or Osteo + Vasculo conditions. However, the BV of the Osteo alone group was significantly higher compared with all other groups. At 8 weeks, both the Blank and Osteo conditions had significantly higher BV compared with the Vasculo and Osteo + Vasculo groups. Evaluation of TMD showed no differences across treatments at the 4-week time point. At the 8-week time point the Blank treatment showed significantly higher TMD compared with the Vasculo or Osteo conditions. Histological analysis and von Kossa staining confirmed the μCT data (Fig. 8), and showed the same trends. Positive mineral staining was evenly distributed throughout the implanted structures in amounts that correlated with the BV calculations.

Discussion

The goal of this study was to evaluate a dual-phase microbead-hydrogel system for promoting bone formation. The osteogenic microbead phase consisted of predifferentiated bmMSC that were embedded in microscale (50–250 μm diameter) COL/FIB/HA modules. The microbeads in turn were distributed within a 3D vasculogenic matrix consisting of a COL/FIB hydrogel containing a bmMSC-HUVEC coculture. Our previous work has demonstrated that microbeads support osteogenic differentiation of bmMSC,[19] and that populations of microbeads can be collected and injected through a needle without the loss of cell viability.[18] Therefore, microbeads can be maintained in culture and exposed to desired differentiation conditions, and they can subsequently be collected and implanted without the need to disrupt the cellular microenvironment. Microbeads also can be combined with other types of biomaterials to create multiphase constructs.[24] In this work, we homogeneously dispersed osteogenically predifferentiated microbeads within a COL/FIB composite hydrogel containing

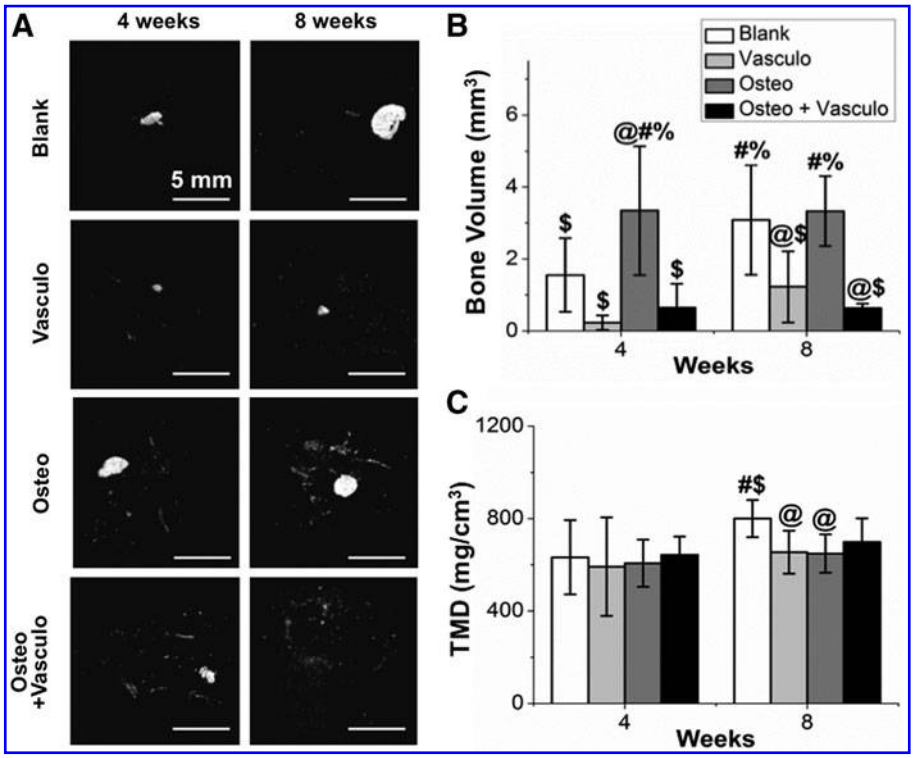

FIG. 7. Microcomputed tomography analysis of ectopic bone formation. Images show **(A)** representative 3D volumetric images of newly formed bone. Graphs show quantification of **(B)** total bone volume and **(C)** tissue mineral density. [@]Statistically significant versus Blank. [#]Statistically significant versus Vasculo. [$]Statistically significant versus Osteo. [%]Statistically significant versus Osteo + Vasculo.

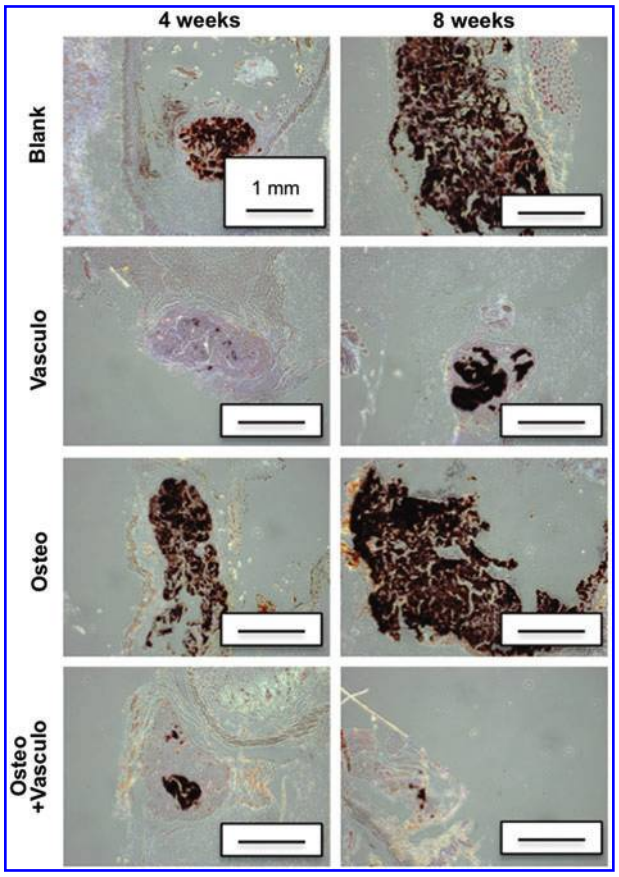

FIG. 8. von Kossa staining of distributed mineral in implants at 4 and 8 weeks. *Black* staining indicates mineralization. Scale bar = 1 mm. Color images available online at www.liebertpub.com/tea

a coculture of bmMSC-HUVEC that we have previously shown to support vasculogenesis *in vitro*.[20] The rationale for combining these phases was to promote simultaneous cellular osteogenesis and neovascularization to enhance the formation of new bone. Human cells were used to evaluate their potential to generate vascularized bone tissue and to maintain clinical relevance. The overall objective of this work is to develop a minimally invasive therapy for treating large and recalcitrant bone defects.

We first investigated vasculogenesis in 3D hydrogel constructs that contained either acellular or osteogenically differentiated cell-seeded microbeads *in vitro*. Robust endothelial cell networks formed in the hydrogel in both conditions containing HUVEC (Osteo + Vasculo, Vasculo). Interestingly, we did not observe an inhibitory effect of including osteogenically differentiated cells into our system on *in vitro* vessel formation. Although there are contradictory reports in the literature,[25] some studies have observed that the differentiated state of cocultured bmMSC can influence vascular network formation by HUVEC.[25] In addition, we did not observe positive staining for endothelial cell markers in osteogenic microbeads when cultured alone, in contrast to reports that have suggested that MSC can differentiate along both osteogenic and vasculogenic cell lineages.[26–29] Taken together, our *in vitro* data provided support that osteogenic microbeads could be used in combination with a vasculogenic outer matrix, without impeding vascular network formation.

We then progressed to a subcutaneous implant model in the mouse to examine bone and blood vessel formation by both mono- and dual-phase constructs. The bmMSC in the osteogenic microbead component were predifferentiated for 2 weeks prior to being combined with an outer hydrogel containing a combination of undifferentiated bmMSC and HUVEC immediately prior to injection. Previous studies have shown that cotransplantation of undifferentiated bmMSC and HUVEC leads to the generation of vascular structures containing human cells in this animal model at 1 and 2 weeks.[22,23] In these studies, MSC were shown to act as pericytes in the neovascularization process and their presence was associated with a more mature and stable vasculature. The subcutaneous location of the implants used in this study allowed angiogenesis from surrounding fat and muscle tissue, thereby generating perfusion of the implant site. The animal model supported the implantation of two constructs per animal, and therefore facilitated contralateral comparisons in this proof-of-concept study.

Noninvasive Doppler imaging showed consistent, above-baseline levels of construct perfusion regardless of the treatment condition, with the exception of the purely vasculogenic condition at 8 weeks, which showed a significant decline in perfusion. However, quantification of neovasculature using histology showed no statistically significant differences between any of the conditions at either time point. These data suggest that while the constructs were well perfused, the inclusion of endothelial cells did not improve vascularization of the implant site. Human endothelial cells were implanted in this study, however, we observed little evidence of human UEA-1 staining in the explanted tissues at 4 or 8 weeks. Previous studies have shown that transplanted human cells are present 1 week after implantation,[22,23] suggesting that transplanted cells participate in generating perfusion, but that they are replaced by host cells over time. The microbeads used in this study also contained exogenous HA, the primary mineral component of bone, which has been shown to have an osteoinductive effect on bmMSC.[30] In addition, HA has shown the ability to promote sprouting of HUVEC,[31,32] and to induce the secretion of the angiogenic growth factor VEGF when presented to bmMSC.[30,33] The dissolution of HA was not monitored in this study, but the HA contained within or released from the microbeads may have provided an angiogenic signal for the host vasculature to infiltrate the implant and support bone formation. In this case, the exogenously supplied HUVEC may not have been needed to achieve perfusion of the implants.

Previous studies using a variety of experimental systems have shown that the combination of endothelial cells with MSC can potentiate bone formation. *In vitro* studies have confirmed that coculture of these cell types can achieve reciprocal beneficial effects: endothelial cells can secrete BMP-2 to serve as osteogenic signal for MSC,[14] which can conversely release VEGF to provide an angiogenic signal for endothelial cells.[34,35] Several studies have shown comparable[36] or increased[37,38] bone formation with the transplantation of both cell types in orthotopic bone regeneration models. Recent studies using ectopic models have yielded either increased[14,17] or equivalent[39,40] bone formation in

the dual cell condition, compared to the osteogenic cell condition alone. In this study, addition of undifferentiated bmMSC in combination with HUVEC exhibited a marked inhibitory effect on ectopic bone formation by osteogenically differentiated microbeads *in vivo*. While the mechanism of action is not evident from these data, the presence of undifferentiated bmMSC in the dual-phase condition may have resulted in paracrine signals that inhibited bone formation.

The results of our study were clear, but it did not support our expectation that a dual-phase osteogenic-vasculogenic tissue construct would enhance bone formation. The complexity of the *in vivo* environment makes it difficult to draw strong mechanistic conclusions from this study, however, modular microbeads represent a leading-edge approach that combine 3D protein biomaterials and multiple cells types for multiphase tissue regeneration, and the data we have presented can guide the work of other groups developing similar approaches. Additional experiments will help illuminate the complex interplay between vasculogenesis and osteogenesis in the implant environment. In addition, we note that this study used commercially sourced bmMSC because they are well characterized for identity and function, however, our findings need to be validated across a larger pool of progenitor cell sources to make the results more generally applicable.

The choice of a subcutaneous ectopic model to examine proof-of-concept of our dual-phase approach is also relevant to interpretation of the results, since it is possible that in this model exogenous cells are not required to achieve neovascularization and mineralization of the implant. Notably, the Blank (acellular) microbead-hydrogel samples resulted in a similar degree of bone formation as the Osteo group, suggesting that the matrix itself may be osteoinductive in this model, through the recruitment of endogenous cells. Therefore, an orthotopic model, in which angiogenesis and cellular recruitment from surrounding tissue is reduced, may be more appropriate for demonstrating the potential of the dual-phase tissue approach. In particular, a dual-phase engineered tissue may be of most value in ischemic bone wounds, in which the host tissue does not have the ability to regenerate the vasculature needed to support bone regeneration. While it is difficult to create a reliable small animal model of ischemic bone repair, our approach may show benefit in larger segmental defects, which typically result in nonunion unless a therapeutic intervention is applied, and where concomitant regeneration of a vasculature is likely to be more important for bone formation. Recent studies have suggested that the processes of neovascularization and bone formation are coupled, though the relationships are not fully understood.[41]

In summary, this study has demonstrated the use of an injectable modular approach that applies COL/FIB/HA microbeads for orthopedic applications. The microbead phase generated robust bone formation in an ectopic model. Contrary to our expectation, the addition of undifferentiated bmMSC and HUVEC as part of the vasculogenic phase had an inhibitory effect on bone formation in this model. The mechanism of inhibition is unclear, but may be related to the presence of undifferentiated bmMSC in proximity to the osteogenic phase. Testing of this approach in a nonunion or ischemic model may illuminate whether endothelial cells and/or bmMSC can potentiate bone healing in recalcitrant wounds. This work provides insight into bone formation by implanted bmMSC, and IT may lead to improved methods for engineering vascularized bone tissue. The microbead-hydrogel approach may have utility in treating large cavitary defects such as tumor resections and avascular necrosis, where transplantation of cells may be needed to fully regenerate lost tissue. Such injectable cell-based therapies would aid in the treatment of a variety of orthopedic pathologies in which bone regeneration is delayed or prevented.

Acknowledgments

This work was supported in part by a National Science Foundation Graduate Research Fellowship (DGE 1256260, to R.R.R.), National Institute of Arthritis and Musculoskeletal and Skin Diseases grants R21-AR062709 and R01-AR062636 (to J.P.S.), and by National Heart, Lung, and Blood Institute grants R01-HL118259 (to A.J.P. and J.P.S.) and R01-HL085339 (to A.J.P.). The authors would like to thank Chris Strayhorn and Theresa Cody at the Histology Core at the University of Michigan School of Dentistry for assistance in processing of histological samples, and Michelle Lynch at the MicroCT Core at the University of Michigan School of Dentistry for help with imaging and analysis of samples.

Disclosure Statement

The authors have no competing financial interests.

References

1. Clarke, B. Normal bone anatomy and physiology. Clin J Am Soc Nephrol **3,** S131, 2008.
2. Buck, D.W., 2nd, and Dumanian, G.A. Bone biology and physiology: Part I. The fundamentals. Plast Reconstr Surg **129,** 1314, 2012.
3. Patel, Z.S., Young, S., Tabata, Y., Jansen, J.A., Wong, M.E., and Mikos, A.G. Dual delivery of an angiogenic and an osteogenic growth factor for bone regeneration in a critical size defect model. Bone **43,** 931, 2008.
4. Young, S., Patel, Z.S., Kretlow, J.D., Murphy, M.B., Mountziaris, P.M., Baggett, L.S., Ueda, H., Tabata, Y., Jansen, J.A., Wong, M., and Mikos, A.G. Dose effect of dual delivery of vascular endothelial growth factor and bone morphogenetic protein-2 on bone regeneration in a rat critical-size defect model. Tissue Eng Part A **15,** 2347, 2009.
5. Shah, N.J., Macdonald, M.L., Beben, Y.M., Padera, R.F., Samuel, R.E., and Hammond, P.T. Tunable dual growth factor delivery from polyelectrolyte multilayer films. Biomaterials **32,** 6183, 2011.
6. Kumar, S., Wan, C., Ramaswamy, G., Clemens, T.L., and Ponnazhagan, S. Mesenchymal stem cells expressing osteogenic and angiogenic factors synergistically enhance bone formation in a mouse model of segmental bone defect. Mol Ther **18,** 1026, 2010.
7. McKay, W.F., Peckham, S.M., and Badura, J.M. A comprehensive clinical review of recombinant human bone morphogenetic protein-2 (INFUSE Bone Graft). Int Orthop **31,** 729, 2007.
8. Carreon, L.Y., Glassman, S.D., Brock, D.C., Dimar, J.R., Puno, R.M., and Campbell, M.J. Adverse events in patients re-exposed to bone morphogenetic protein for spine surgery. Spine **33,** 391, 2008.
9. Shahlaie, K., and Kim, K.D. Occipitocervical fusion using recombinant human bone morphogenetic protein-2: adverse

effects due to tissue swelling and seroma. Spine **33,** 2361, 2008.
10. Epstein, N.E. Pros, cons, and costs of INFUSE in spinal surgery. Surg Neurol Int **2,** 10, 2011.
11. Nguyen, L.H., Annabi, N., Nikkhah, M., Bae, H., Binan, L., Park, S., Kang, Y., Yang, Y., and Khademhosseini, A. Vascularized bone tissue engineering: approaches for potential improvement. Tissue Eng Part B Rev **18,** 363, 2012.
12. Liu, Y., Chan, J.K., and Teoh, S.H. Review of vascularised bone tissue-engineering strategies with a focus on co-culture systems. J Tissue Eng Regen Med 2012 [Epub ahead of print]; doi: 10.1002/term.1617.
13. Rao, R.R., and Stegemann, J.P. Cell-based approaches to the engineering of vascularized bone tissue. Cytotherapy **15,** 1309, 2013.
14. Kaigler, D., Krebsbach, P.H., West, E.R., Horger, K., Huang, Y.C., and Mooney, D.J. Endothelial cell modulation of bone marrow stromal cell osteogenic potential. FASEB J **19,** 665, 2005.
15. Usami, K., Mizuno, H., Okada, K., Narita, Y., Aoki, M., Kondo, T., Mizuno, D., Mase, J., Nishiguchi, H., Kagami, H., and Ueda, M. Composite implantation of mesenchymal stem cells with endothelial progenitor cells enhances tissue-engineered bone formation. J Biomed Mater Res A **90,** 730, 2009.
16. Grellier, M., Granja, P.L., Fricain, J.C., Bidarra, S.J., Renard, M., Bareille, R., Bourget, C., Amédée, J., and Barbosa, M.A. The effect of the co-immobilization of human osteoprogenitors and endothelial cells within alginate microspheres on mineralization in a bone defect. Biomaterials **30,** 3271, 2009.
17. Tsigkou, O., Pomerantseva, I., Spencer, J.A., Redondo, P.A., Hart, A.R., O'Doherty, E., Lin, Y., Friedrich, C.C., Daheron, L., Lin, C.P., Sundback, C.A., Vacanti, J.P., and Neville, C. Engineered vascularized bone grafts. Proc Natl Acad Sci U S A **107,** 3311, 2010.
18. Wang, L., Rao, R.R., and Stegemann, J.P. Delivery of mesenchymal stem cells in chitosan/collagen microbeads for orthopedic tissue repair. Cells Tissues Organs **197,** 333, 2013.
19. Rao, R.R., Peterson, A.W., and Stegemann, J.P. Osteogenic differentiation of adipose-derived and marrow-derived mesenchymal stem cells in modular protein/ceramic microbeads. J Biomed Mater Res A **101,** 1531, 2013.
20. Rao, R.R., Peterson, A.W., Ceccarelli, J., Putnam, A.J., and Stegemann, J.P. Matrix composition regulates three-dimensional network formation by endothelial cells and mesenchymal stem cells in collagen/fibrin materials. Angiogenesis **15,** 253, 2012.
21. Gudur, M., Rao, R.R., Hsiao, Y.S., Peterson, A.W., Deng, C.X., and Stegemann, J.P. Noninvasive, quantitative, spatiotemporal characterization of mineralization in three-dimensional collagen hydrogels using high-resolution spectral ultrasound imaging. Tissue Eng Part C Methods **18,** 935, 2012.
22. Grainger, S.J., Carrion, B., Ceccarelli, J., and Putnam, A.J. Stromal cell identity influences the *in vivo* functionality of engineered capillary networks formed by co-delivery of endothelial cells and stromal cells. Tissue Eng Part A **19,** 1209, 2013.
23. Kniazeva, E., Kachgal, S., and Putnam, A.J. Effects of extracellular matrix density and mesenchymal stem cells on neovascularization *in vivo*. Tissue Eng Part A **17,** 905, 2011.
24. Caldwell, D.J., Rao, R.R., and Stegemann, J.P. Assembly of discrete collagen-chitosan microenvironments into multiphase tissue constructs. Adv Healthc Mater **2,** 673, 2013.
25. Thébaud, N.B., Siadous, R., Bareille, R., Remy, M., Daculsi, R., Amédée, J., and Bordenave, L. Whatever their differentiation status, human progenitor derived—or mature—endothelial cells induce osteoblastic differentiation of bone marrow stromal cells. J Tissue Eng Regen Med **6,** e51, 2012.
26. Janeczek Portalska, K., Leferink, A., Groen, N., Fernandes, H., Moroni, L., van Blitterswijk, C., and de Boer, J. Endothelial differentiation of mesenchymal stromal cells. PLoS One **7,** e46842, 2012.
27. Zhang, R., Gao, Z., Geng, W., Yan, X., Chen, F., and Liu, Y. Engineering vascularized bone graft with osteogenic and angiogenic lineage differentiated bone marrow mesenchymal stem cells. Artif Organs **36,** 1036, 2012.
28. Mihaila, S.M., Frias, A.M., Pirraco, R.P., Rada, T., Reis, R.L., Gomes, M.E., and Marques, A.P. Human adipose tissue-derived SSEA-4 subpopulation multi-differentiation potential towards the endothelial and osteogenic lineages. Tissue Eng Part A **19,** 235, 2013.
29. Correia, C., Grayson, W., Eton, R., Gimble, J.M., Sousa, R.A., Reis, R.L., and Vunjak-Novakovic, G. Human adipose-derived cells can serve as a single-cell source for the *in vitro* cultivation of vascularized bone grafts. J Tissue Eng Regen Med **8,** 629, 2014.
30. He, J., Genetos, D.C., and Leach, J.K. Osteogenesis and trophic factor secretion are influenced by the composition of hydroxyapatite/poly(lactide-co-glycolide) composite scaffolds. Tissue Eng Part A **16,** 127, 2010.
31. Rücker, M., Laschke, M.W., Junker, D., Carvalho, C., Tavassol, F., Mülhaupt, R., Gellrich, N.C., and Menger, M.D. Vascularization and biocompatibility of scaffolds consisting of different calcium phosphate compounds. J Biomed Mater Res A **86,** 1002, 2008.
32. Pezzatini, S., Solito, R., Morbidelli, L., Lamponi, S., Boanini, E., Bigi, A., and Ziche, M. The effect of hydroxyapatite nanocrystals on microvascular endothelial cell viability and functions. J Biomed Mater Res A **76,** 656, 2006.
33. He, J., Decaris, M.L., and Leach, J.K. Bioceramic-mediated trophic factor secretion by mesenchymal stem cells enhances *in vitro* endothelial cell persistence and *in vivo* angiogenesis. Tissue Eng Part A **18,** 1520, 2012.
34. Kaigler, D., Krebsbach, P.H., Polverini, P.J., and Mooney, D.J. Role of vascular endothelial growth factor in bone marrow stromal cell modulation of endothelial cells. Tissue Eng **9,** 95, 2003.
35. Li, Q., and Wang, Z. Influence of mesenchymal stem cells with endothelial progenitor cells in co-culture on osteogenesis and angiogenesis: an *in vitro* study. Arch Med Res **44,** 504, 2013.
36. Koob, S., Torio-Padron, N., Stark, G.B., Hannig, C., Stankovic, Z., and Finkenzeller, G. Bone formation and neovascularization mediated by mesenchymal stem cells and endothelial cells in critical-sized calvarial defects. Tissue Eng Part A **17,** 311, 2011.
37. Seebach, C., Henrich, D., Kähling, C., Wilhelm, K., Tami, A.E., Alini, M., and Marzi, I. Endothelial progenitor cells and mesenchymal stem cells seeded onto beta-TCP granules enhance early vascularization and bone healing in a critical-sized bone defect in rats. Tissue Eng Part A **16,** 1961, 2010.

38. Kim, J.Y., Jin, G.Z., Park, I.S., Kim, J.N., Chun, S.Y., Park, E.K., Kim, S.Y., Yoo, J., Kim, S.H., Rhie, J.W., and Cho, D.W. Evaluation of solid free-form fabrication-based scaffolds seeded with osteoblasts and human umbilical vein endothelial cells for use *in vivo* osteogenesis. Tissue Eng Part A **16,** 2229, 2010.
39. Fedorovich, N.E., Haverslag, R.T., Dhert, W.J., and Alblas, J. The role of endothelial progenitor cells in prevascularized bone tissue engineering: development of heterogeneous constructs. Tissue Eng Part A **16,** 2355, 2010.
40. Geuze, R.E., Wegman, F., Oner, F.C., Dhert, W.J., and Alblas, J. Influence of endothelial progenitor cells and platelet gel on tissue-engineered bone ectopically in goats. Tissue Eng Part A **15,** 3669, 2009.
41. Uhrig, B.A., Boerckel, J.D., Willett, N.J., Li, M.T., Huebsch, N., and Guldberg, R.E. Recovery from hind limb ischemia enhances rhBMP-2-mediated segmental bone defect repair in a rat composite injury model. Bone **55,** 410, 2013.

Address correspondence to:
Jan P. Stegemann, PhD
Department of Biomedical Engineering
University of Michigan
1101 Beal Avenue
Ann Arbor, MI 48109

E-mail: jpsteg@umich.edu

Received: December 5, 2013
Accepted: September 4, 2014
Online Publication Date: October 16, 2014

This article has been cited by:

1. Ramkumar Tiruvannamalai Annamalai, Ana Y. Rioja, Andrew J. Putnam, Jan P. Stegemann. 2016. Vascular Network Formation by Human Microvascular Endothelial Cells in Modular Fibrin Microtissues. *ACS Biomaterials Science & Engineering* **2**:11, 1914-1925. [Crossref]
2. Joel K. Wise, Andrea I. Alford, Steven A. Goldstein, Jan P. Stegemann. 2016. Synergistic enhancement of ectopic bone formation by supplementation of freshly isolated marrow cells with purified MSC in collagen–chitosan hydrogel microbeads. *Connective Tissue Research* **57**:6, 516-525. [Crossref]
3. Sonja B. Riemenschneider, Donald J. Mattia, Jacqueline S. Wendel, Jeremy A. Schaefer, Lei Ye, Pilar A. Guzman, Robert T. Tranquillo. 2016. Inosculation and perfusion of pre-vascularized tissue patches containing aligned human microvessels after myocardial infarction. *Biomaterials* **97**, 51-61. [Crossref]
4. Lucia Forte, Paola Torricelli, Elisa Boanini, Massimo Gazzano, Katia Rubini, Milena Fini, Adriana Bigi. 2016. Antioxidant and bone repair properties of quercetin-functionalized hydroxyapatite: An in vitro osteoblast–osteoclast–endothelial cell co-culture study. *Acta Biomaterialia* **32**, 298-308. [Crossref]
5. Ramkumar Tiruvannamalai Annamalai, David R. Mertz, Ethan L.H. Daley, Jan P. Stegemann. 2016. Collagen Type II enhances chondrogenic differentiation in agarose-based modular microtissues. *Cytotherapy* **18**:2, 263-277. [Crossref]
6. Xanthippi Chatzistavrou, Rameshwar R. Rao, David J. Caldwell, Alexis W. Peterson, Blake McAlpin, Yuan-Yuan Wang, Li Zheng, J. Christopher Fenno, Jan P. Stegemann, Petros Papagerakis. 2016. Collagen/fibrin microbeads as a delivery system for Ag-doped bioactive glass and DPSCs for potential applications in dentistry. *Journal of Non-Crystalline Solids* **432**, 143-149. [Crossref]